SUPPORTING INFORMATION

Chinese Journal of Structural Chemistry

Selective Electrocatalytic Hydrogenation of 5-Hydroxymethyl-furfural to 2,5-Dihydroxymethylfuran on Bimetallic PdCu Alloy

Xu Yue[1], Weixing Zhao[1], Shuangyin Wang[1] and Yuqin Zou[1,2]*

[1]*State Key Laboratory of Chem/Bio-Sensing and Chemometrics, College of Chemistry and Chemical Engineering, Advanced Catalytic Engineering Research Center of the Ministry of Education, Hunan University, Changsha 410082, China*

[2]*Shenzhen Institute of Hunan University, Shenzhen 518057, China*

Corresponding author. Email: yuqin_zou@hnu.edu.cn

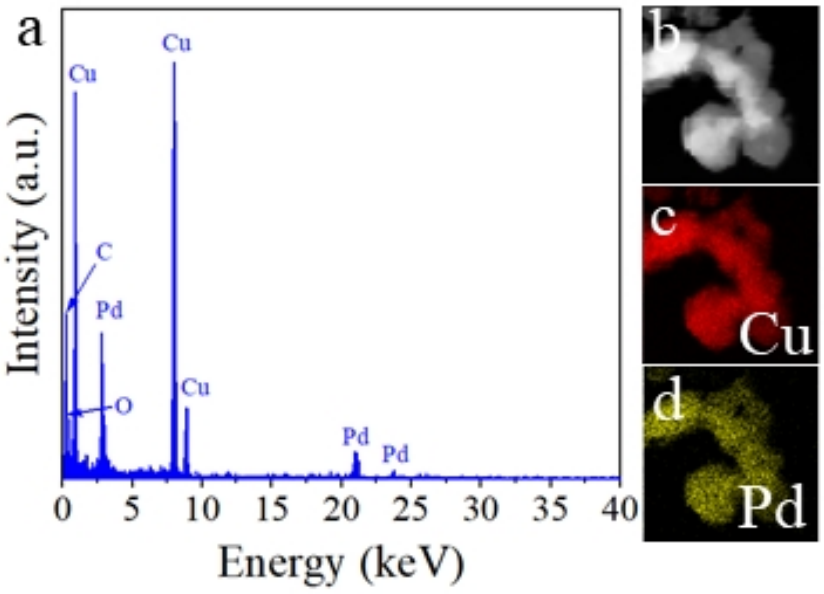

Figure S1. a) TEM-EDS pattern of $Pd_{0.3}Cu$. b~d) EDS elemental mapping images of $Pd_{0.3}Cu$.

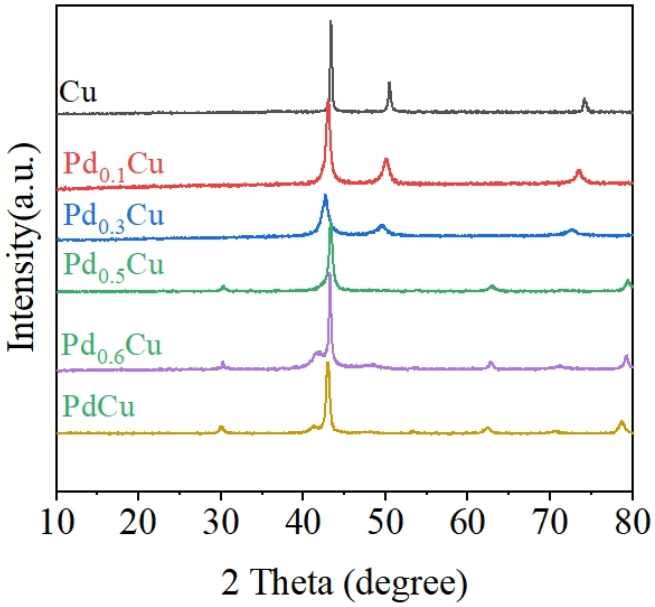

Figure S2. XRD patterns of Cu nanoparticles: Pd0.1Cu, Pd0.3Cu, Pd0.5Cu, Pd0.6Cu, and PdCu.

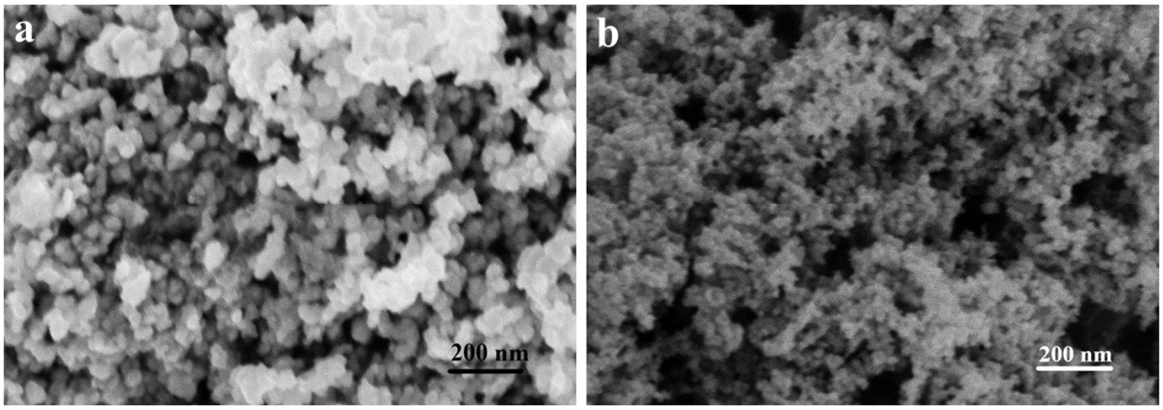

Figure S3. SEM images of Cu nanoparticles and b) Pd nanoparticles.

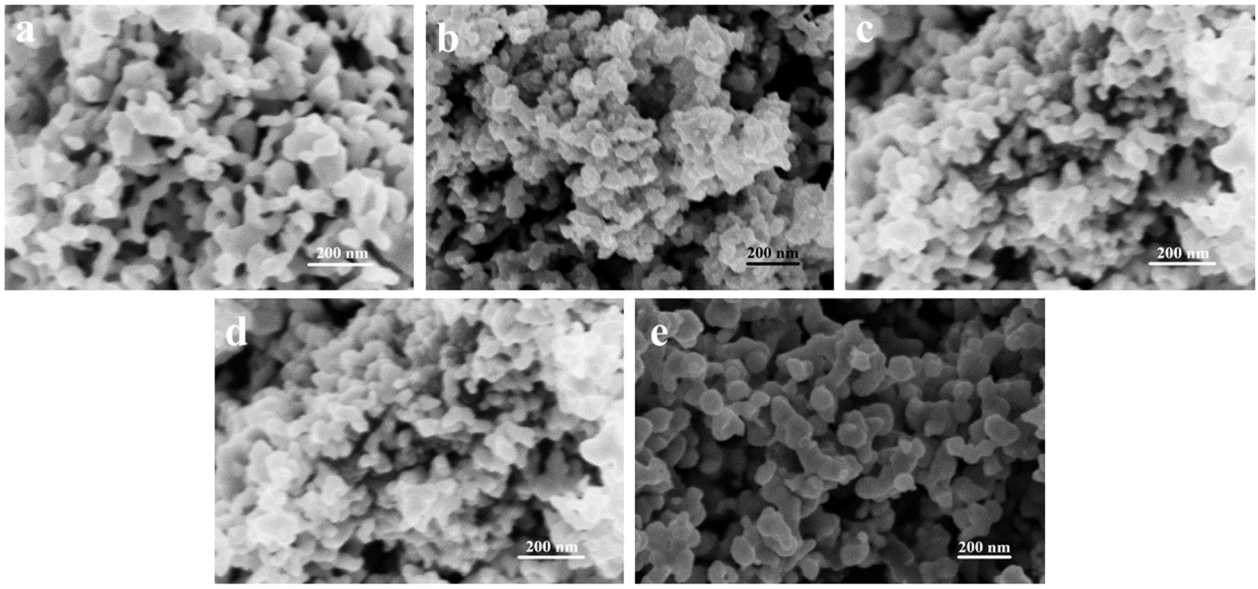

Figure S4. SEM images of a) $Pd_{0.1}Cu$, b) $Pd_{0.3}Cu$, c) $Pd_{0.5}Cu$, d) $Pd_{0.6}Cu$ and e) PdCu.

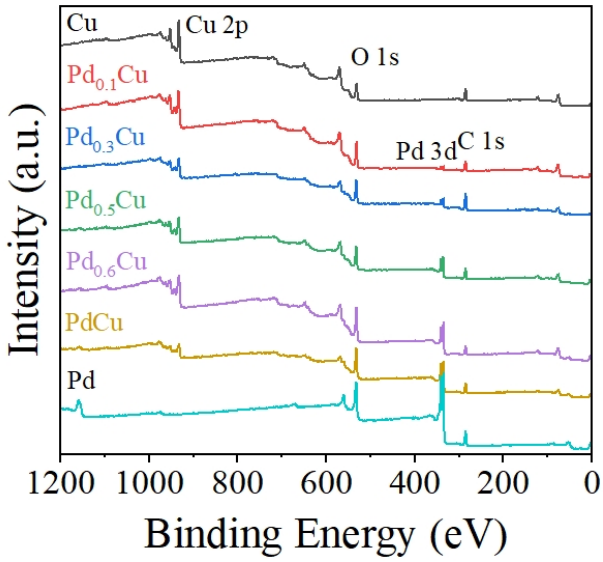

Figure S5. XPS survey spectra of Pd nanoparticles, Cu nanoparticles, $Pd_{0.1}Cu$, $Pd_{0.3}Cu$, $Pd_{0.5}Cu$, $Pd_{0.6}Cu$ and PdCu.

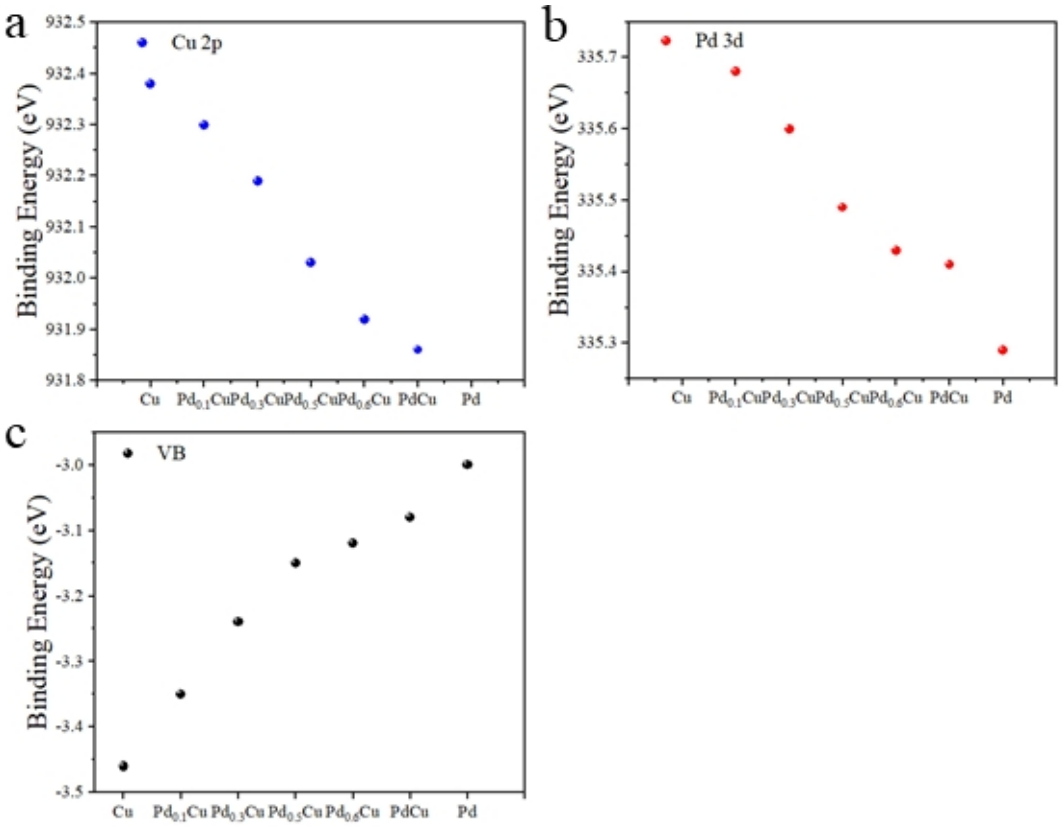

Figure S6. The binding energy of Cu^0 $2p_{3/2}$, Pd^0 $3d_{5/2}$ and d-bond center of Pd_xCu.

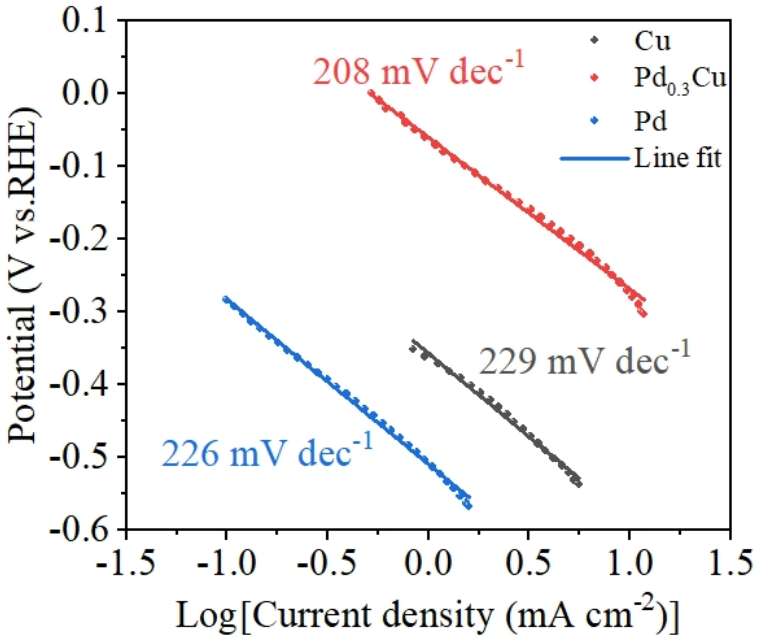

Figure S7. Tafel slopes of Cu nanoparticles, $Pd_{0.3}Cu$ and Pd nanoparticles.

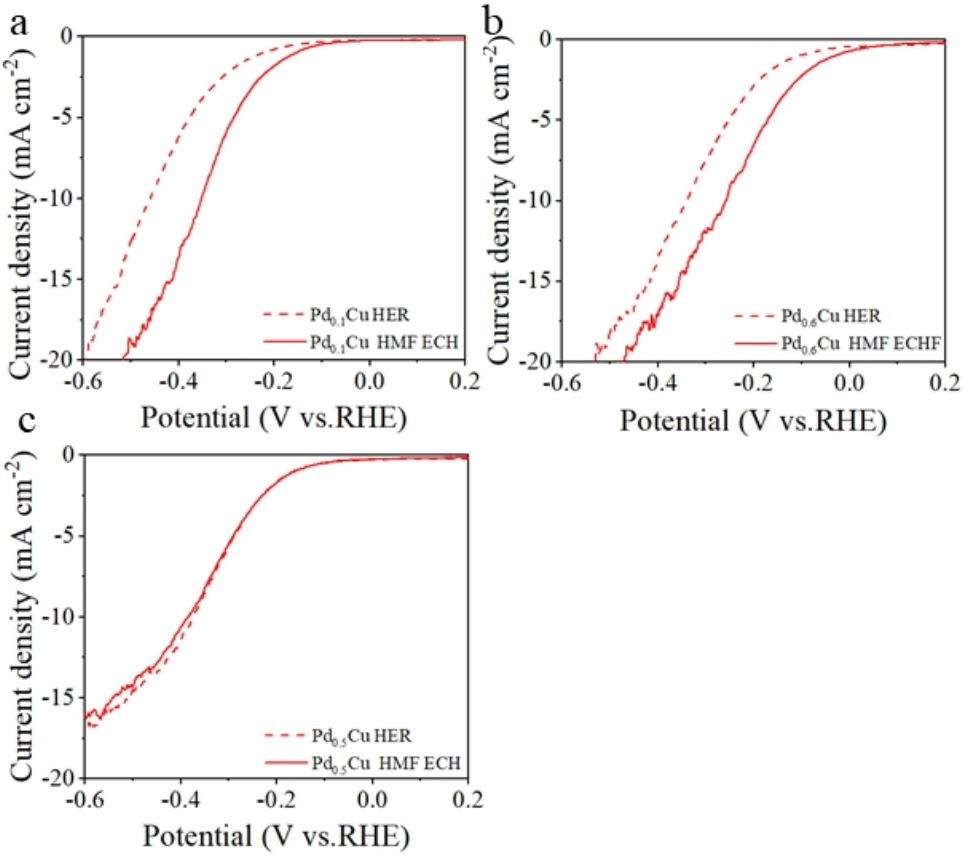

Figure S2. LSV curves of a) $Pd_{0.1}Cu$, b) $Pd_{0.5}Cu$ and c) $Pd_{0.6}Cu$ in PBS without and with HMF.

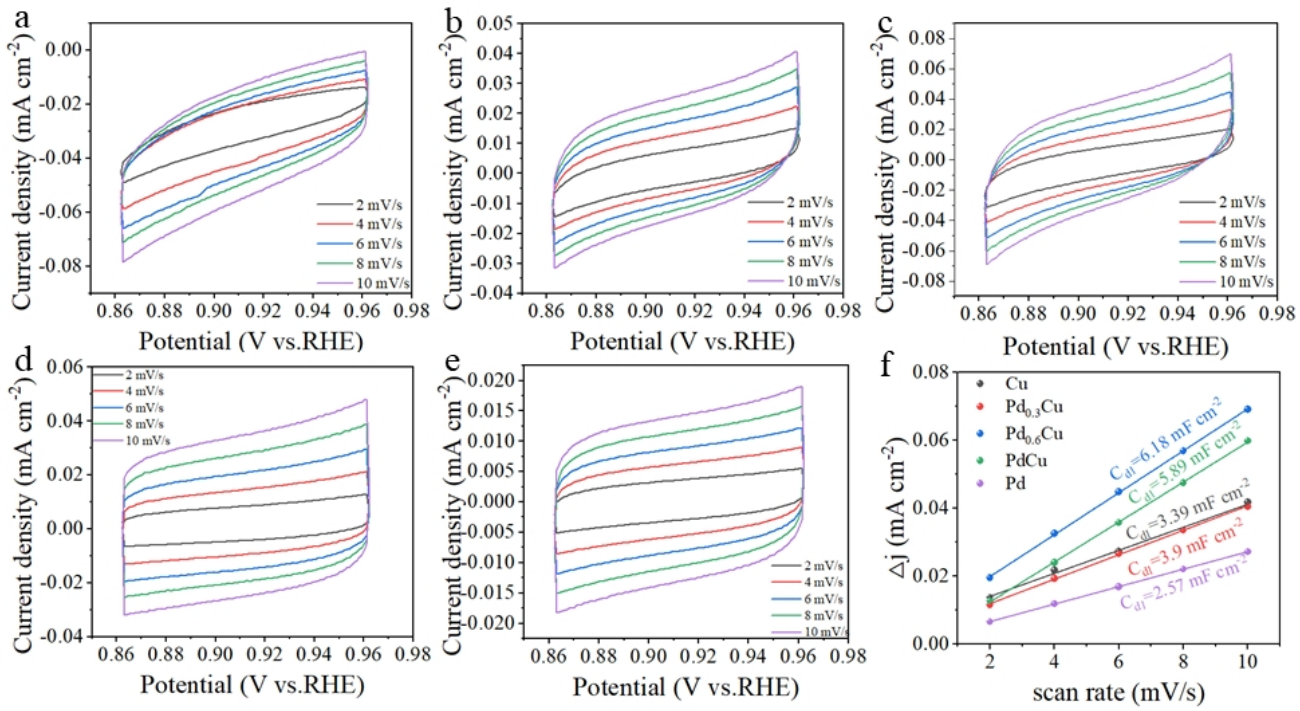

Figure S9. CV curves for (a) Cu nanoparticles; (b) $Pd_{0.3}Cu$; (c) $Pd_{0.6}Cu$; (d) PdCu; (e) Pd; at different scan rates: 2, 4, 6, 8 and 10 mV s^{-1} from inside to outside. (f) Capacitive currents at 0.91 V (vs. RHE) as a function of the scan rate for Cu nanoparticles, $Pd_{0.3}Cu$, $Pd_{0.6}$ Cu, PdCu and Pd.

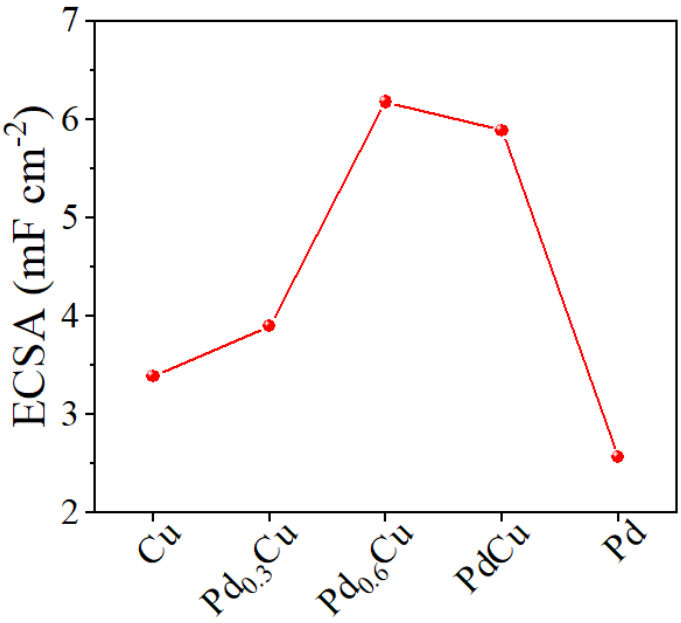

Figure S3. The relationship between the ECSA and the contents of Pd and Cu.

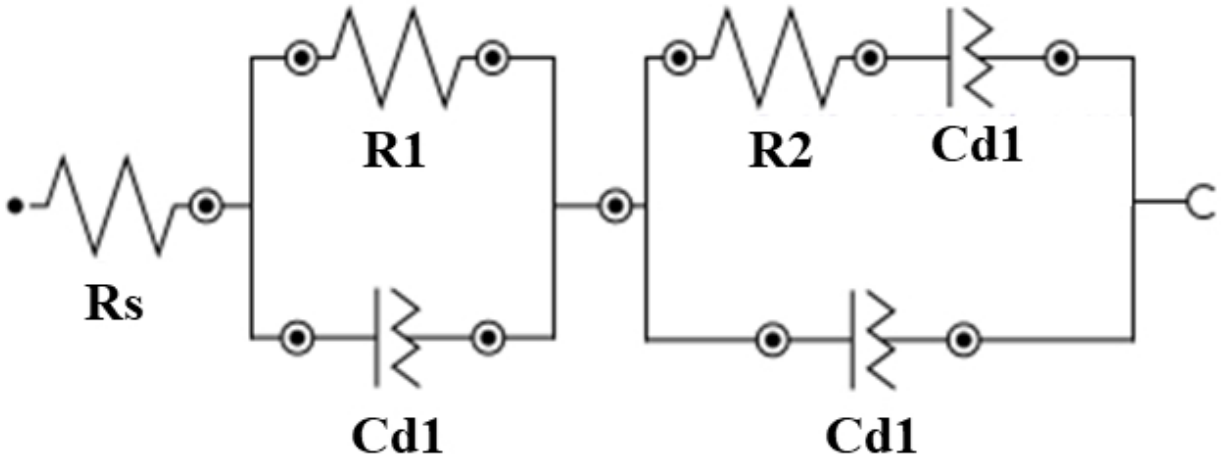

Figure S4. The equivalent circuit used for modeling the measured electrochemical response. Rs stands for the solution resistance, Cdl represents double layer capacitance, and Rp has contact with the interfacial charge transfer reaction.

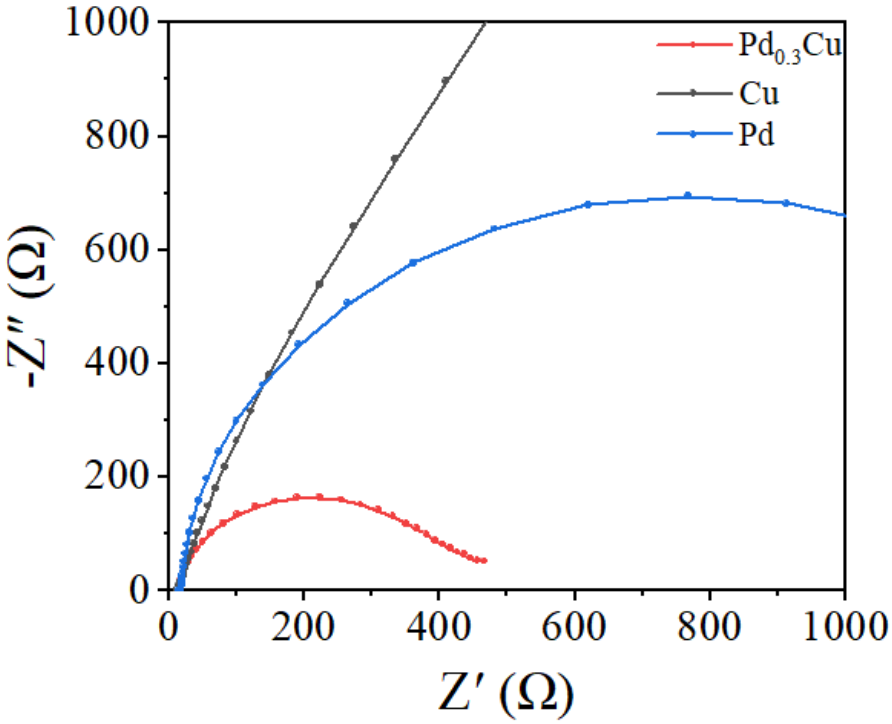

Figure S5. Nyquist plots for Cu nanoparticles, $Pd_{0.3}Cu$ and Pd nanoparticle catalysts in PBS with HMF at -0.15 V (vs. RHE).

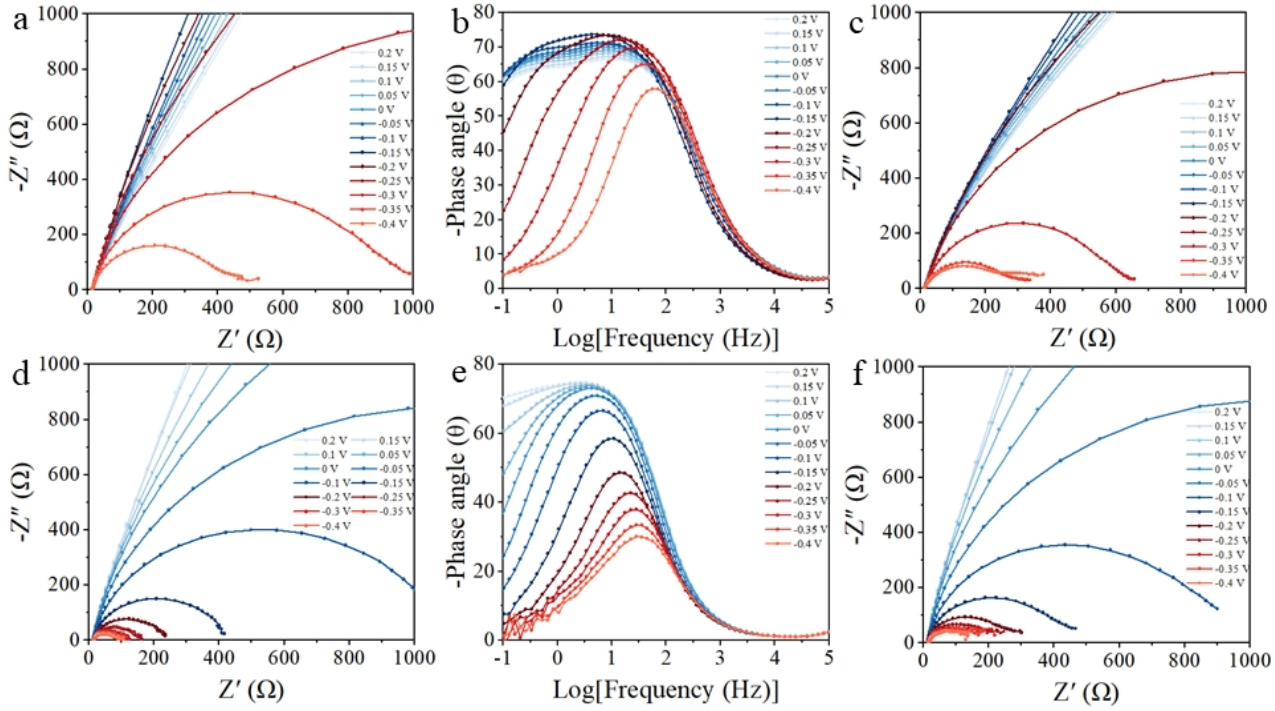

Figure S6. a) Operando Nyquist and b) Bode phase plots of Cu nanoparticles at various applied potentials in 1.0 M PBS; c) Operando Nyquist and d) Bode phase plots of Cu nanoparticles at various applied potentials in M PBS with HMF.

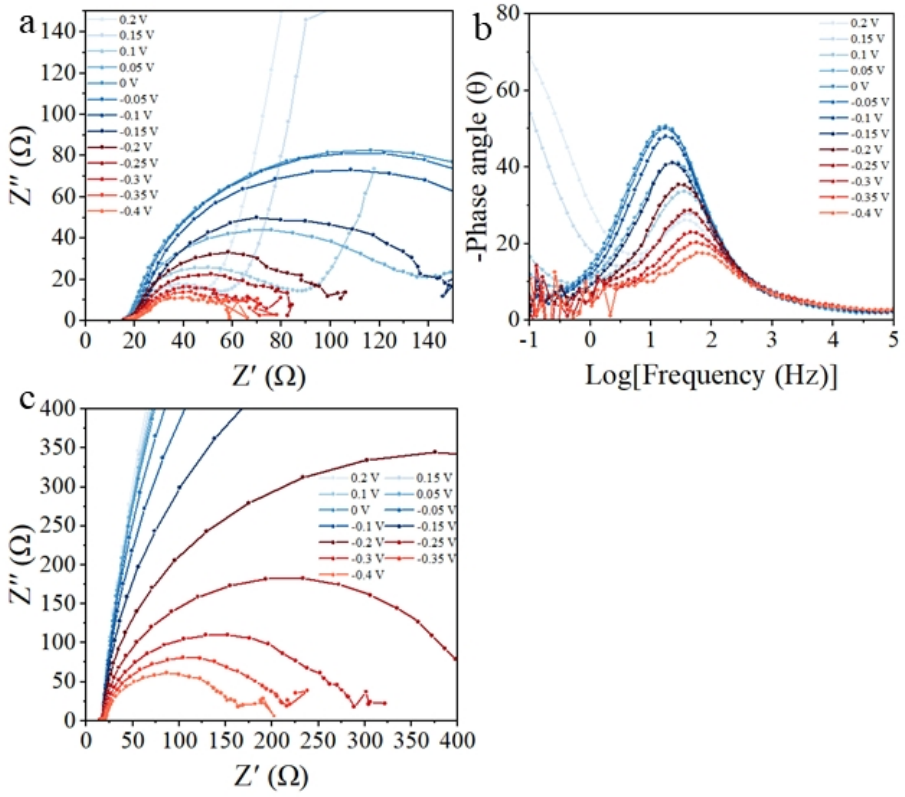

Figure S7. Operando Nyquist and Bode phase plots of $Pd_{0.3}Cu$ at various applied potentials in PBS a) without and b) with HMF.

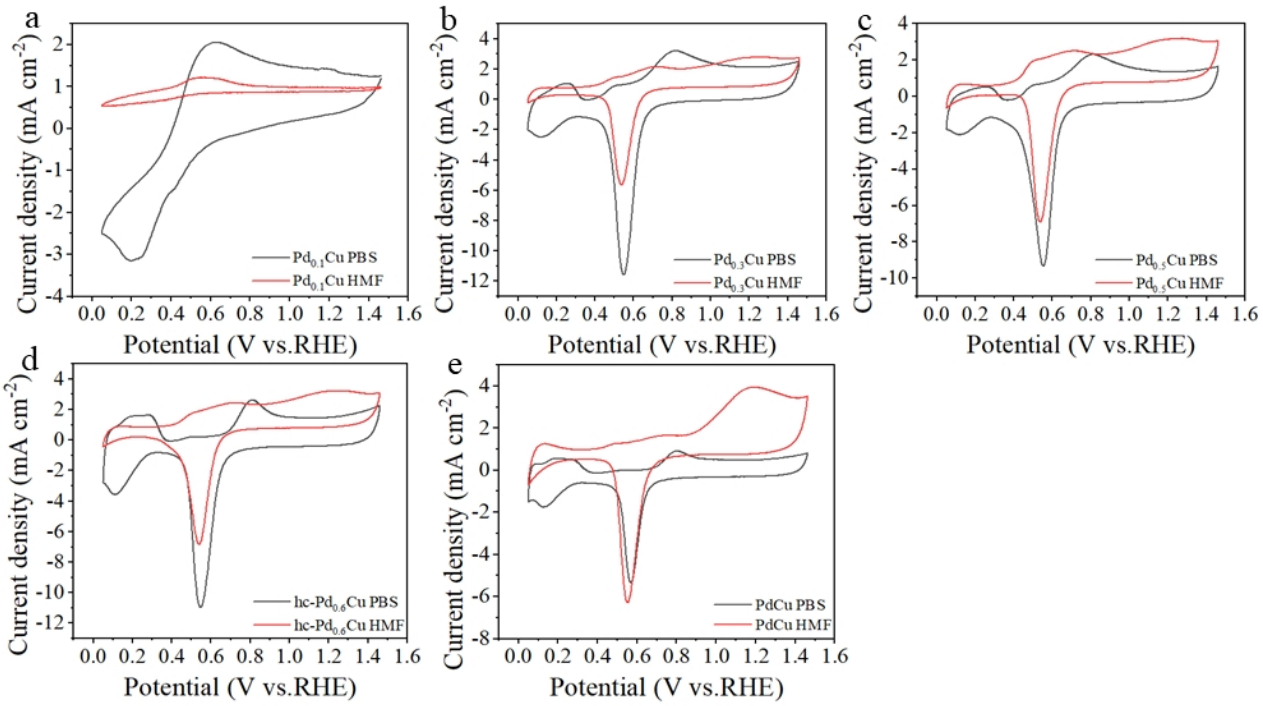

Figure S8. Cyclic voltammetry of a) $Pd_{0.1}Cu$, b) $Pd_{0.2}Cu$, c) $Pd_{0.3}Cu$, d) $Pd_{0.4}Cu$, e) $Pd_{0.5}Cu$, f) $Pd_{0.6}Cu$ and g) PdCu in PBS solution with and without HMF. h) Cyclic voltammetry of Pd*x*Cu alloys in PBS solution with HMF.

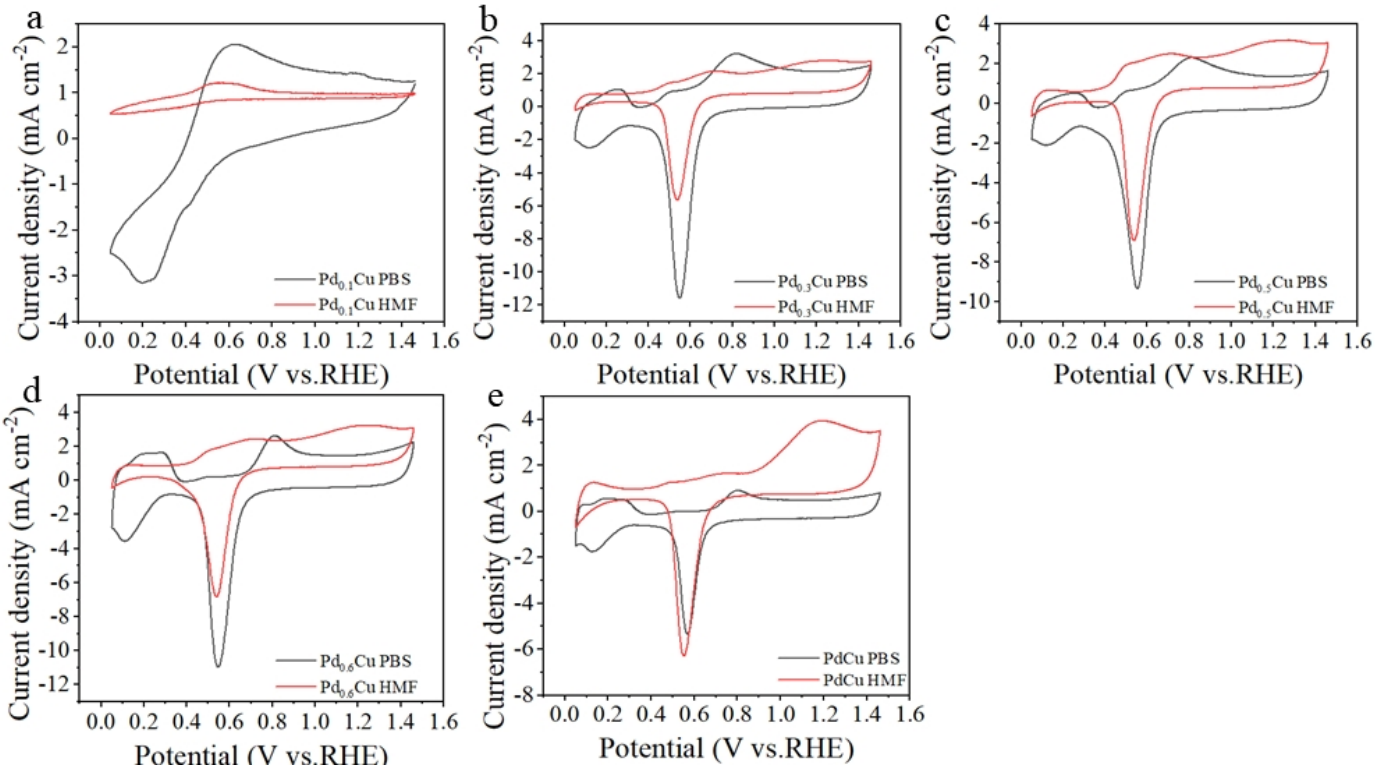

Figure S16. Cyclic voltammetry of a) $Pd_{0.1}Cu$, b) $Pd_{0.3}Cu$, c) $Pd_{0.5}Cu$, d) $Pd_{0.6}Cu$ and e) PdCu in PBS solution with and without HMF"

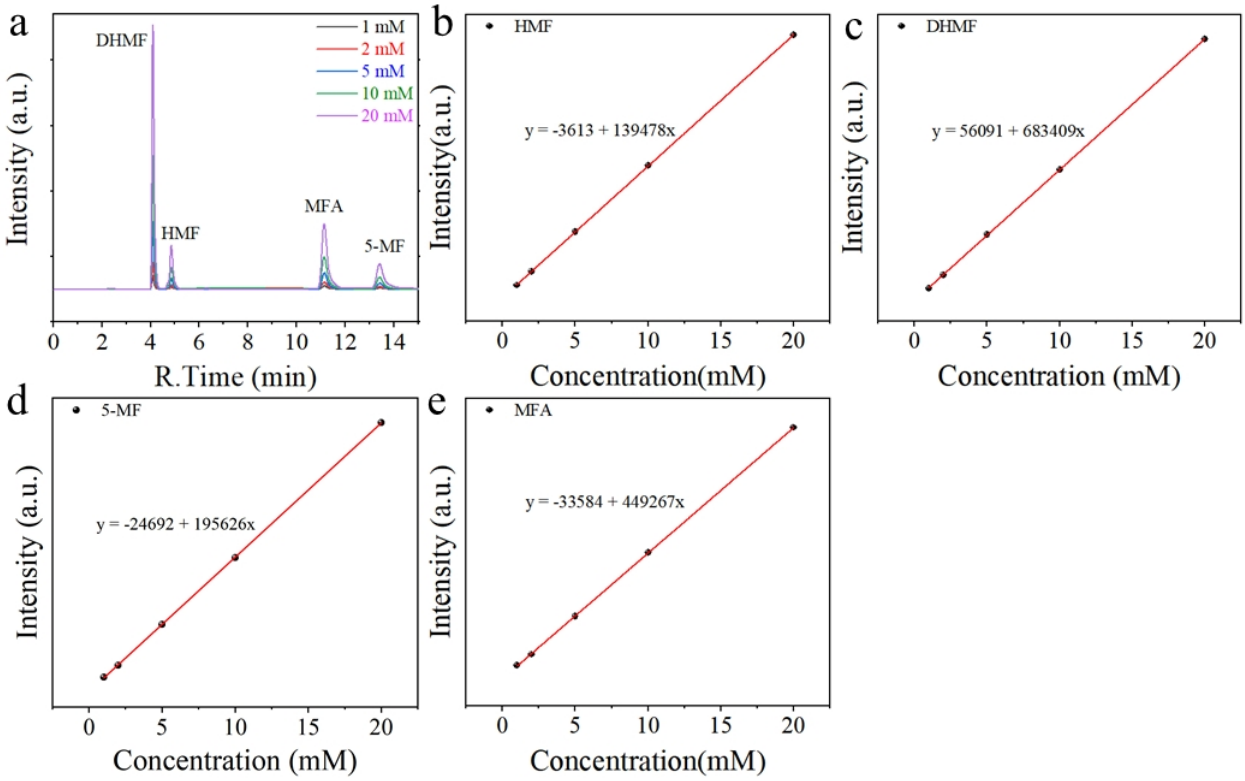

Figure S9. a) HPLC chromatograms of HMF, DHMF, MFA and 5-MF. Calibrations of the HPLC for b) HMF, c) DHMF, d) MFA and e) 5-MF.

Table S1. Summary of the Impedance of Cu Nanoparticles and $Pd_{0.3}Cu$ in 1.0 M PBS Electrolyte Obtained by Fitting with an Equivalent Circuit that Consisted of Electrolyte Resistance (Rs), Charge-transfer Resistance (Rp) and Double-layer Capacitance (Cdl)

Samples	Cu nanoparticles	Ordered $CuPd_{0.3}$	Pd
Rs	12.395	14.177	14.737
R1	2092	151.6	1469.8
R2	235.6	40.402	154.2

Table S2. Comparison of Electrolysis Performance of Catalysts for HMF Hydrogenation

Electrocatalyst	Onset potential	Product (selectivity)	Conversion	Ref.
$Pd_{0.3}Cu$	-0.05 V	DHMF (99%)	89%	This work
8%ZrO_2-doped graphite	-1 V	DMF (30.7%)		[1]
Ag_{gd}	-0.22 V	DHMF	99%	[2]
Ag_{sp}	-0.3 V		84%	
Cu	-0.26 V		39%	
Ag-displaced nano textured Cu	-0.31 V	DHMF (92%)	98%	[3]
CuNi bimetallic alloy	-0.25 V	DMF (91.1%)		[4]
Pd/VN/CF	-0.04 V	DHMTHF (92%)	87%	[5]
Ag/C	0.31 V	DHMF (96.2%)	70%	[6]
Ag electrodeposited on Cu open-cell foams	-0.24 V	DHMF (99%)	93%	[7]

n REFERENCES

(1) Yu, X.; Wen, Y.; Yuan, T.; Li, G. Effective production of 2,5-dimethylfuran from biomass-derived 5-hydroxymethylfurfural on ZrO_2-doped graphite electrode. *Chemistryselect* **2017**, 2, 1237-1240.

(2) Roylance, J. J.; Kim, T. W.; Choi, K. S. Efficient and selective electrochemical and photoelectrochemical reduction of 5-hydroxymethylfurfural to 2,5-bis(hydroxymethyl)furan using water as the hydrogen source. *Acs Catalysis* **2016**, 6, 1840-1847.

(3) Zhang, L.; Zhang, F.; Michel, F. C. Jr.; Co, A. C. Efficient electrochemical hydrogenation of 5-hydroxymethylfurfural to 2,5-bis(hydroxymethyl)furan on Ag-displaced nanotextured cu catalysts. *Chemelectrochem* **2019**, 6, 4739-4749.

(4) Zhang, Y. R.; Wang, B. X.; Qin, L.; Li, Q.; Fan, Y. M. A non-noble bimetallic alloy in the highly selective electrochemical synthesis of the biofuel 2,5-dimethylfuran from 5-hydroxymethylfurfural. *Green Chem.* **2019**, 21, 1108-1113.

(5) Li, S.; Sun, X.; Yao, Z.; Zhong, X.; Coo, Y.; Liang, Y.; Wei, Z.; Deng, S.; Zhuang, G.; Li, X.; Wang, J. Biomass valorization via paired electrosynthesis over vanadium nitride-based electrocatalysts. *Adv. Funct. Mater.* **2019**, 29, DOI: 10.1002/adfm.201904780.

(6) Chadderdon, X. H.; Chadderdon, D. J.; Pfennig, T.; Shanks, B. H.; Li, W. Paired electrocatalytic hydrogenation and oxidation of 5-(hydroxymethyl)furfural for efficient production of biomass-derived monomers. *Green Chem.* **2019**, 21, 6210-6219.

(7) de Luna, G. S.; Ho, P. H.; Lolli, A.; Ospitali, F.; Albonetti, S.; Fornasari, G.; Benito, P. Ag electrodeposited on cu open-cell foams for the selective electroreduction of 5-hydroxymethylfurfural. *Chemelectrochem* **2020**, 7, 1238-1247.